http://dx.doi.org/10.5012/bkcs.2012.33.5.1753

Enhancement in the Photocatalytic Activity of Au@TiO_2 Nanocomposites by Pretreatment of TiO_2 with UV Light

Mohammad Mansoob Khan, Shafeer Kalathil, Jintae Lee, and Moo Hwan Cho*

School of Chemical Engineering, Yeungnam University, Gyeongsan, Gyeonsangbukdo 712-749, Korea
**E-mail: mhcho@ynu.ac.kr*
Received January 18, 2012, Accepted February 27, 2012

A novel, efficient and controlled protocol for the synthesis and enhanced photocatalytic activity of Au@TiO_2 nanocomposite is developed. TiO_2 (P25) was pretreated by employing UV light ($\lambda = 254$ nm) and the pretreated TiO_2 was uniformly decorated by gold nanoparticles (AuNPs) in presence of sodium citrate and UV light. UV pretreatment makes the TiO_2 activated, as electrons were accumulated within the TiO_2 in the conduction band. These accumulated electrons facilitate the formation of AuNPs which were of very small size (2-5 nm), similar morphology and uniformly deposited at TiO_2 surface. It leads to formation of stable and crystalline Au@TiO_2 nanocomposites. The rapidity (13 hours), monodispersity, smaller nanocomposites and easy separation make this protocol highly significant in the area of nanocomposites syntheses. As-synthesized nanocomposites were characterized by TEM, HRTEM, TEM-EDX, SAED, XRD, UV-visible spectrophotometer and zeta potential. Dye degradation experiments of methyl orange show that type I (Au@TiO_2 nanocomposites in which TiO_2 was pretreated with UV light) has enhanced photocatalytic activity in comparison to type II (Au@TiO_2 nanocomposites in which TiO_2 was not pretreated with UV light) and TiO_2 (P25). This shows that pretreatment of TiO_2 provides type I a better catalytic activity.

Key Words : Au@TiO_2, Nanocomposites, Pretreatment, Photocatalyst, UV-light

Introduction

Gold has been considered as a fairly inert metal. However, gold at nano scale behave entirely different than the bulk material. It was established by Haruta[1,2] and Bond[3] a few decades ago by showing that, when gold is dispersed as small nanoparticles, it can catalyze several hydrogenation and oxidation reactions.

Gold/metal-oxide nanocomposites have become one of the scorching topics in catalysis, being widely used to many important reactions, such as CO oxidation, nitrogen oxide reduction, selective oxidation of propene, and photocatalytic oxidations.[3-6] It has been confirmed by various studies that the catalytic property of Au/metal-oxide nanocomposites depends significantly on the size of AuNPs, interaction between Au and the supporting oxide, as well as the nanostructure of the active sites.[2,3,7] This is particularly true for the case of gold catalysts anchored on titania, a support of interest because of its synergistic effect in further facilitating the promotion of oxidation[8-10] and photocatalytic reactions.[10-12] For gold supported catalysts, different supports have been intensively explored, and their cooperative effects with gold particles were also explored.[13,14] Among them, TiO_2 is a prominent one due to its easy availability, low-cost, stability and nontoxicity.[15] Recent investigations on gold-TiO_2 nanocomposite also show that gold-doping improves the photocatalytic activity and extends the response of the TiO_2 catalyst into visible region.[16]

Recent research suggests that Au@TiO_2 can be exploited in organic reactions as catalyst,[4,17-19] dye degradation,[10] degradation of phenolic compounds[10] and hydrogen production.[10,15,20] These applications could be more applicable if it expands towards the visible region of the spectrum. It is well established[10,20] that it could be achieved by deposition/doping metal oxides surface especially TiO_2 by noble metals such as Au, Ag *etc*.[21] The effect of pre-thermal treatment of TiO_2 is reported.[22] However, the pretreatment of TiO_2 by UV light before deposition of gold nanoparticles has not yet been documented. There are reports that upon pretreatment of TiO_2 electrons will get accumulated within the semiconductors.[23,24] To inspired with this we decided to use these accumulated electrons for the reduction of Au^{3+} at the surface of pretreated TiO_2. Here our emphasis is to modify/activate the TiO_2 by UV pretreatment and then deposit monodispersed AuNPs with small size by enhancing the rate of the reduction of Au^{3+} at TiO_2 surface.

Herein, we report an efficient synthesis and characterization of Au@TiO_2 nanocomposites using UV light ($\lambda = 254$ nm) as a tool to pretreat the TiO_2 and then deposit the AuNPs at the pretreated TiO_2 in presence of sodium citrate and UV light. Irradiation makes the overall process fast in comparison to other reported methods.[10,25-28] To the best of our knowledge, this is the first protocol to pretreat the TiO_2 by UV light and then uniformly deposit small size and similar shape of AuNPs at the pretreated TiO_2 in aqueous medium at 30 °C. But there are several reports that simultaneous UV irradiation at mixture of $HAuCl_4$ and TiO_2 affords Au@TiO_2.[23,26-30] The as-synthesized nanocomposites was tested for photocatalytic activity to degrade methyl orange.

Experimental

Materials. TiO_2 (P25; Degussa), chloroauric acid ($HAuCl_4 \cdot nH_2O$) (n = 3.6; Kojima Chemical, Japan), sodium citrate ($Na_3C_6H_5O_7 \cdot 2H_2O$) (Duksan Pharmaceutical Co. Ltd. South Korea), extra pure NaOH and methyl orange (Duksan Pure Chemicals Co. Ltd. South Korea) was used as received. Deionized water was prepared in our laboratory by using PURE ROUP 30 water purification system.

Methods. UV lamp (Vilber Lourmat, 4 W, 230 V, 50-60 Hz, λ = 254 nm) was used to pretreat the TiO_2 and irradiate the reaction mixture. The as-synthesized catalysts were characterized by using UV-visible spectrophotometer (UV-1800, Shimadzu, Japan) and powder X-ray diffraction (XRD) was measured on PANalytical, X'Pert-PRO MPD with Cu Kα radiation (λ = 0.15405 nm). Diffraction peaks of crystalline phases were compared with those of standard compounds reported in the JCPDS data file. The gold particle size of the sample was measured by TEM and HRTEM (Tecnai G2 F20, FEI, USA) operating at an accelerating voltage of 200 kV equipped with energy-dispersive X-ray (EDX) analysis system. Nanocomposites were dispersed in ethanol and were sonicated for ten minutes by sonicator (BRANSON 5510) for TEM studies. Selected-area electron diffraction (SAED) images were recorded by the TEM instrument. The zeta potential of the Au@TiO_2 nanocomposites in aqueous solution were determined by using a Delsa™ Nano zeta potential (Beckman Coulter, USA).

Synthesis of Au@TiO_2 Nanocomposites. Au@TiO_2 catalysts were prepared by wet chemical method using $HAuCl_4 \cdot nH_2O$ (n = 3.6) as the gold precursor and commercially available TiO_2 in aqueous solution at 30 °C. Sodium citrate was used as a reducing agent to reduce the Au^{3+} to Au^0. The UV light source used was 4 W UV lamp, wavelength 254 nm. The irradiation time ranges from 3 hours to 20 hours with a stirring speed of 770 rpm. Two different types of Au@TiO_2 nanocomosites were synthesized following similar methodology except the time of irradiation and amount of UV light irradiated. Molar concentration of TiO_2 and gold precursor ($HAuCl_4$) was 2:1. In type I TiO_2 was pretreated by UV light while in type II, there was no pretreatment of TiO_2. Our main focus will be on type I as it is a new protocol. Type II was control sample and it was compared with type I.

Type I: In this case, 5 mM TiO_2 was dispersed in 200 mL DI water and pretreated with UV light (λ = 254 nm) for 3 hours. To this solution, 2.5 mM $HAuCl_4$ was added dropwise and pH 9 was maintained by using 0.1 M NaOH. Color of the reaction mixture was whitish-golden yellow. Then 0.1 g sodium citrate was added and N_2 gas was sparged for 5 minutes to maintain the inert atmosphere. The reaction mixture was sealed and left for stirring with UV irradiation for 10 hours. At the end the color of the reaction mixture changed to brownish-purple with some precipitation.

Type II: In this reaction, 5 mM TiO_2 was dispersed in 200 mL DI water then 2.5 mM $HAuCl_4$ was added drop wise and pH 9 was maintained by using 0.1 M NaOH. Color of the reaction mixture was whitish-golden yellow. Then 0.1 g sodium citrate was added and N_2 gas was sparged for 5 minutes. The reaction mixture was sealed and left for stirring with UV irradiation for 20 hours. At the end the color of the reaction mixture changed to golden-brown with some precipitation.

At the completion of the reaction UV-visible absorbance was measured and absorption band was observed at 547 nm for type I and 537 nm for type II (Figure 4) which is the characteristic absorbance of Au@TiO_2. The product formed in the type I and II was filtered off and repeatedly washed with DI water till all the Cl^- was removed. The color of the isolated product in type I was brownish-purple and in type II was golden-brown. Colorless filtrate was obtained in both the cases which show the completion of the reaction.

Photocatalytic Activity. Photocatalytic experiments were performed as reported previously on methyl orange.[30,31] In short, 13 mg of methyl orange was dissolved in 1000 mL of water and used for photocatalytic activity experiments. 20 mL of methyl orange solution was taken in vials and 5 mg of each catalyst (type I and type II) was added and irradiated with UV light of 254 nm wavelength for 4 hours. The original color degraded. Rate of degradation of the dye was monitored by UV-visible measurement of the reaction mixture at every 30 minutes by taking 1.5 mL of sample from each reaction vial, centrifuged and absorption was measured at 465 nm. Simultaneously, two set of blank experiments using TiO_2 and dye with UV irradiation and dye with UV irradiation were performed to see the combine effect of TiO_2 and UV light on the dye and the only effect of UV light on the dye, respectively. Combine effect of TiO_2 and UV light on the dye were observed but UV light alone did not show any degradation of the dye.

Results and Discussions

The morphology of the Au@TiO_2 nanocomposites was determined by TEM at low magnification as shown in Figure 1(a) and 2(a) for type I and II respectively. It illustrates that the size of as-synthesized Au@TiO_2 nanocomposites are in 20-30 nm range, highly monodispersed and discrete.[32,33] Figure 1(b) and 2(b) shows respective representative HR-TEM images of individual Au@TiO_2 for type I and II respectively. HRTEM image also shows the size of deposited AuNPs on TiO_2 surface which are in the range of 2-5 nm in type I and 15-25 nm in type II. In type I nanocomposites the AuNPs are of very small size (2-5 nm) with similar morphology and are uniformly deposited. In type II the size of deposited AuNPs are bigger than the type I and not uniformly deposited. The possible reason is that in type II, TiO_2 was not pretreated with UV light. From this it appears that pretreatment of TiO_2 helps to get small size, similar morphology and uniform deposition of AuNPs at TiO_2 surface. Similar TEM and HRTEM images were reported earlier for Au@TiO_2 nanocomposites synthesized by various methods.[32,34] Selected-area electron diffraction (SAED) of type I and II are shown in Figure 1(c), and 2(c) respectively, which clear-

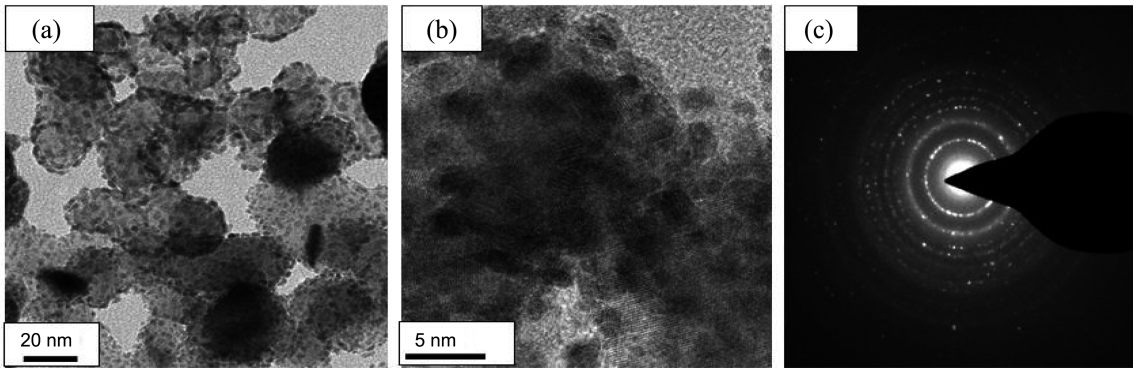

Figure 1. Type I sample (a) TEM micrographs of Au@TiO$_2$ nanocomposites (b) HRTEM of Au@TiO$_2$ nanocomposites demonstrate that very small size (2-5 nm) AuNPs are uniformly anchored at the surface of TiO$_2$ and are not agglomerated (c) SAED of Au@TiO$_2$ nanocomposites showing diffraction cycles.

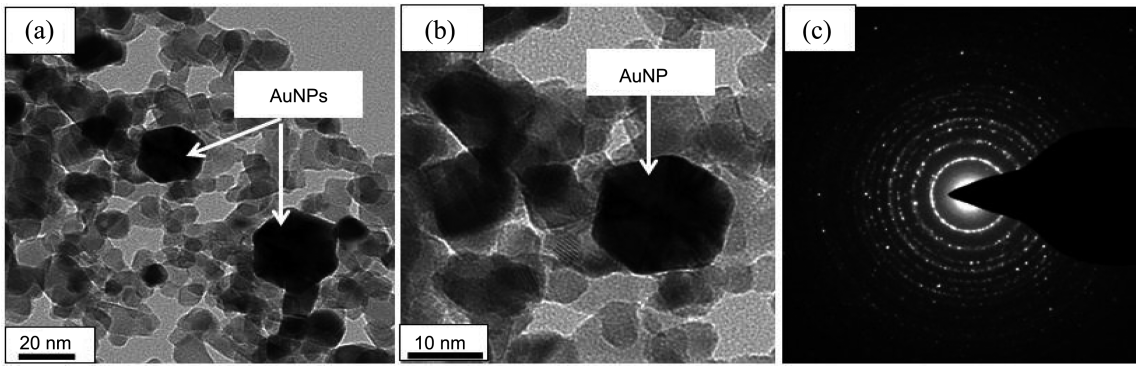

Figure 2. Type II sample (a) TEM micrographs of Au@TiO$_2$ nanocomposites (b) HRTEM of Au@TiO$_2$ nanocomposites demonstrate that AuNPs are anchored at the surface of TiO$_2$ and (c) SAED of Au@TiO$_2$ nanocomposites showing diffraction cycles.

ly show well resolved lattice fringes, diffraction cycles and are indicative of a highly crystalline nature of the as-synthesized nanocomposites. It further confirmed the characteristic crystal planes of Au@TiO$_2$ which are concomitant with the XRD studies (Figure 3).[32] To identify the element composition, an energy-dispersive x-ray (EDX) was employed with an accelerating voltage of 200 kV. It confirms the presence of element gold at TiO$_2$ surface (data not shown).

The phase of the as-synthesized Au@TiO$_2$ nanocomposites

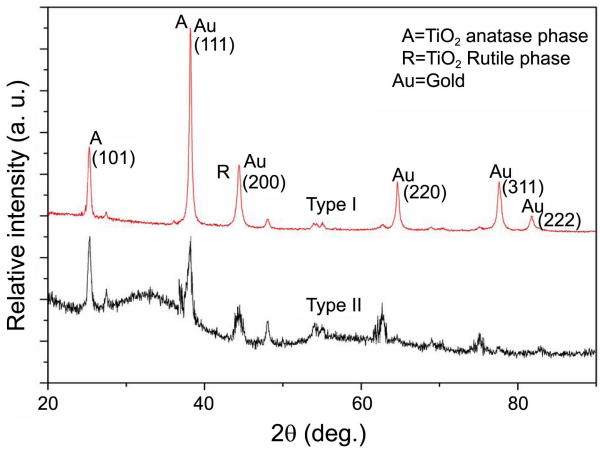

Figure 3. X-ray diffraction (XRD) pattern of Au@TiO$_2$ nanocomposites of type I and II.

was determined by x-ray diffractometry (PANalytical, X'Pert-PRO MPD) with Cu Kα radiation. Figure 3 shows representative X-ray diffraction (XRD) pattern of type I and II Au@TiO$_2$ nanocomposites and confirmed its crystalline nature. XRD pattern shows the prominent diffraction peaks for planes of polycrystalline gold and TiO$_2$ (anatase and rutile phase). Some of the peaks of gold are overlapped with the peaks of TiO$_2$. The XRD pattern also confirmed the formation of metallic gold at the surface of TiO$_2$ as well as overall formation of Au@TiO$_2$ nanocomposite and its crystalline nature. In each type of Au@TiO$_2$ nanocomposite, the cubic lattice of crystalline gold peaks was detected in the patterns from the (111), (200), (220), (311) and (222) reflections. From the XRD spectra, it is also clear that type I is more crystalline than type II. Henceforth, it can be concluded that the crystallinity was found to increase slightly with the pretreatment of TiO$_2$ and pretreatment also enhances formation of small size of AuNPs at TiO$_2$ surface. Calculated d-spacing value at 2θ = 25.2130 and 38.0322 is 3.53230 A^o and 2.36604 A^o observed for TiO$_2$ and AuNPs respectively which are their characteristic values [JCPDS powder diffraction file no. 21-1272]. Similar XRD patterns have been previously reported for Au@TiO$_2$ nanocomposites with average size of ~20 nm.[26,31,35] The average of all the AuNPs peaks in the XRD spectra were used to calculate the average crystallite size by using the Scherrer equation and

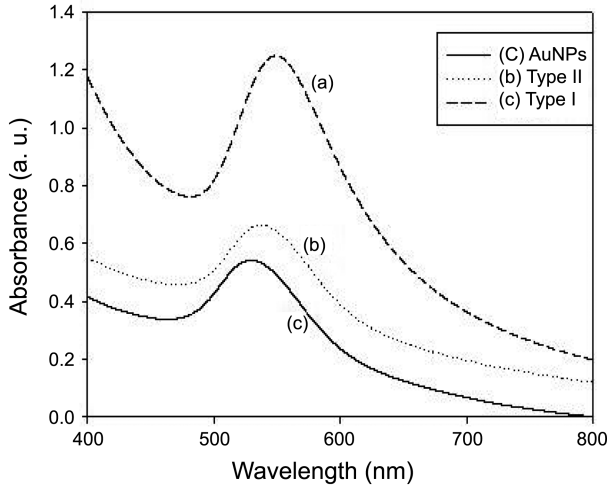

Figure 4. UV-visible spectra of (a) Type I (b) Type II (c) AuNPs.

the full width at half maximum (fwhm).[34,36] The calculated average size of the AuNPs in type I was 6 nm and type II was 25 nm which are very close to TEM and HRTEM values.[36]

UV-visible spectroscopic measurement of the dispersed aqueous solution was recorded and shown in Figure 4. AuNPs was synthesized to compare its surface plasmon band with Au@TiO_2 nanocomposites. It was synthesized as per reported method and its absorption maxima were observed at 529 nm as shown in Figure 4(c).[37] For Au@TiO_2 nanocomposites the appearance of absorbance maximum for type I was at 547 nm (Figure 4(a)) and type II was at 537 nm (Figure 4(b)), which are typically ascribed to the surface plasmon absorbance of Au@TiO_2. It indicates the formation of almost spherical AuNPs at TiO_2 surface.[33,35] It is well known that as the concentration of gold on titania increases the surface plasmon absorbance bands shifts towards higher wave length.[27,35] It is clear from Figure 4 that bands were red shifted for nanocomposites as the concentration of deposited AuNPs on TiO_2 surface has increased. This also indicates an interaction between the gold nanoparticles and the titania support.[35] According to Mie theory, metal nanoparticles like Au will show a surface plasmon band within the range of 500-550 nm.[38] Similar UV spectra for monodispersed nanocomposites system have been already reported.[27,39,40]

The zeta potential of the Au@TiO_2 nanocomposites in aqueous solution were measured which reveals that a surface potential of +38.21 mV for type I and +6.16 mV for type II implying that Au@TiO_2 are positively charged. Type I was showing high zeta potential value, which indicate its stability in solution.[27] From the zeta potential values it also appears that as the amount of deposited AuNPs on TiO_2 surface is increasing the charge of overall nanocomposite is also increasing. The following Scheme 1 was proposed which shows the activation of TiO_2 by pretreatment of UV light and anchoring of AuNPs at the pretreated surface of TiO_2.[10,24,32]

The results of the above characterization techniques reveal that pretreatment of TiO_2 by irradiation of UV light activates and modifies the TiO_2 as shown in Scheme 1. During irradiation of TiO_2 the electrons in the valance band get excited and accumulated within the TiO_2 particles.[24] Then in the presence of sodium citrate, UV light, and pretreated TiO_2, reduction of Au^{3+} to Au^0 was enhanced which leads to small size and similar shape of AuNPs uniformly deposited at the surface of pretreated TiO_2. It makes this protocol interesting and unique in case of type I compared to type II nanocomposite. In type II, mixture of TiO_2 and gold precursor were irradiated together while in type I, TiO_2 was pretreated with UV light and then the mixture of TiO_2 and gold precursor were irradiated again with UV light. The pretreatment helps in the small size, similar morphology and uniform distribution of AuNPs at the surface of pretreated TiO_2.

Photocatalytic Activity. The photocatalytic activity experiment for type I, II and TiO_2 (P25, Degussa) were performed by the photodegradation of methyl orange in aqueous solution by UV light irradiation at room temperature. Methyl orange is a photostable dye and it cannot be photodegraded in the absence of any catalyst under UV or visible light irradiation.[31] Pure TiO_2 (P25) was used as a reference photocatalyst in the photodegradation experiments.

Figure 5(a) shows comparative degradation of methyl orange by type I, II and TiO_2 catalysts under UV light irradiation for 4 hours. The average degradation in terms of percentage of methyl orange in a solution can be calculated

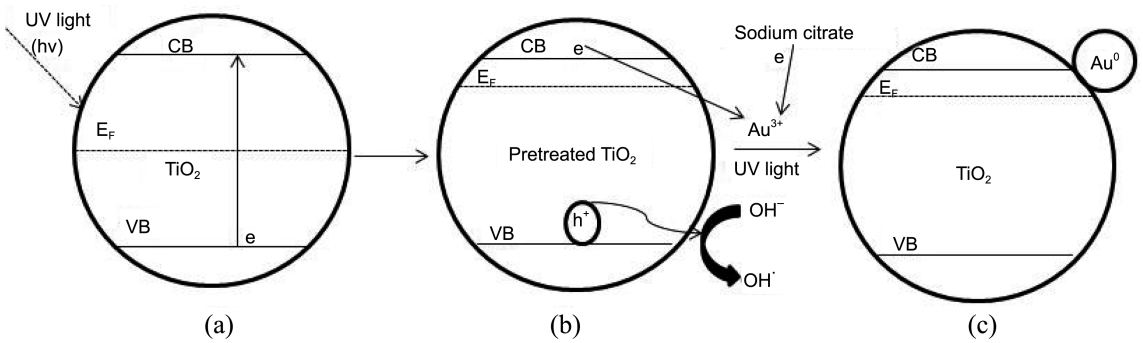

Scheme 1. Proposed mechanism for the formation of Au@TiO_2 nanocomposites (type I). (a) Pretreatment of TiO_2 surface by UV light (b) Pretreated TiO_2 helps in the reduction of Au^{3+} to Au^0 with sodium citrate as electron donor and holes formed are scavenged by OH^- (c) As-synthesized Au@TiO_2 nanocomposites.

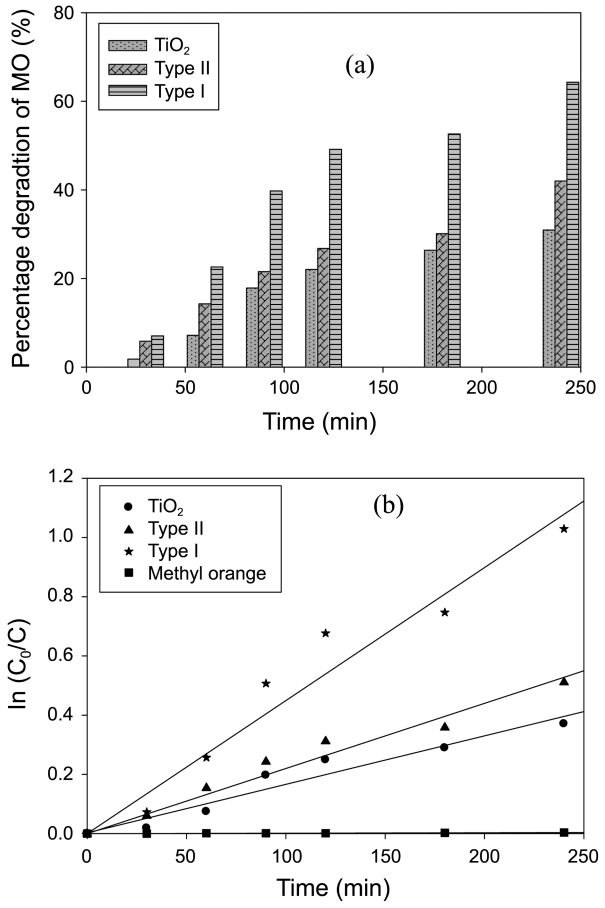

Figure 5. Photocatalytic activity of type I, II and TiO_2 (P25) (a) Degradation of methyl orange by type I, II and TiO_2 in terms of percentage (b) Graph fitted with linearity from which the rate constants were determined.

by using the following formula:

$$\eta = \left[\frac{A_0 - A_t}{A_0}\right] \times 100\% \quad (1)$$

where η is the degradation rate of methyl orange in terms of percentage, t is the reaction time, A_0 and A_t are the initial and relic methyl orange concentration, respectively.[41] It was observed that type I shows higher catalytic activity than type II and pure TiO_2. Figure 5(b) shows a plot of $\ln(C_o/C)$ *vs.* time for type I, II, TiO_2 and methyl orange. The photocatalytic activity for all the samples was quantitatively evaluated by calculating the respective pseudo first-order rate constants (k) according to the following equation:

$$ln\left(\frac{C_o}{C}\right) = kt \quad (2)$$

where C_o and C are the initial concentration and the reaction concentration of methyl orange at time t, respectively.[42] The graphs were fitted with linearity from which the rate constants (k) were determined. Rate constant for type I, k_I was 7.48×10^{-5} sec^{-1}, type II, k_{II} was 3.66×10^{-5} sec^{-1} and TiO_2, k_{TiO2} was 2.73×10^{-5} sec^{-1}. The rate constant represents the photocatalytic activity of the samples. The higher the rate constant value, the faster the degradation of methyl orange and thus better the photocatalytic activity of the samples.

From this it seems that photocatalytic activity depends on the preparation method and the gold loading on TiO_2. This finding suggests that crystallinity of the nanocomposites and particle size of deposited AuNPs plays important role in determining the photocatalytic activity. It is also supported by our XRD data and TEM studies.[43] From this, it was concluded that pretreatment of TiO_2 provides type I enhanced photocatalytic activity as compared to type II where pretreatment was not given to TiO_2.

From the above discussion and scheme it is clear that, the electrons (having energies > 3.02 eV, band gap energy of TiO_2) were excited from valence band to conduction band by using the UV light of 254 nm and accumulated in the conduction band of TiO_2.[24] Finally, distribution of electrons takes place between the pretreated TiO_2 and Au^{3+} to facilitate the formation of AuNPs provided that they are in close contact.[44] Here the role of pretreated TiO_2 and sodium citrate are to act as reducing agent by providing electrons to Au^{3+} to reduce Au^0. This leads to the formation of uniform, similar morphology and small size of AuNPs at the surface of TiO_2. The holes formed in the TiO_2 will migrate to the electrolyte interface and are scavenged by the OH^- ions as shown in Scheme 1.[29] From the above discussion it is also clear that TiO_2 serves dual purpose, as a support for AuNPs and facilitating the formation of gold nanoparticles by providing electrons that were stored in the conduction band. In type I Au@TiO_2 nanocomposite, pretreatment of TiO_2 facilitate the formation of very small size (2-5 nm), similar morphology and uniformly deposited AuNPs at the surface of TiO_2 as it was clear from TEM and HRTEM micrographs. In comparison to type I, type II shows different pattern, because in this case pretreatment was not given to TiO_2. This is in good agreement with the observation of the present protocol that Au@TiO_2 nanocomposites have very small size (2-5 nm) of deposited AuNPs at the surface of pretreated TiO_2 which has imparted it an enhanced and unique catalytic property. The photocatalytic degradation of methyl orange shows that type I where size of deposited AuNPs was in the range of 2-5 nm, has better degradation than type II, where the size of AuNPs was in the range of 15-25 nm. Similar results about the size-dependent catalytic properties of AuNPs deposited on titania have been obtained in earlier studies.[3,4]

The advantage of our synthetic protocol is that we employed DI water as a solvent which does not have any adverse effect on the environment. Our protocol does not involve any expensive device or materials except UV lamp. The Au@TiO_2 nanocomposites obtained are highly stable in the reaction mixture as well as after isolation from reaction mixture in solid state to air and moisture which allows its smooth handling for various further applications. Moreover, it is a controlled synthesis. As it is already established that the size and morphology of gold nanoparticles may affect its reactivity.[3,8,20,44] Therefore, from the dye degradation experi-

ments it was observed that the newly synthesized nanocomposites (type I) shows enhanced photocatalytic activity compared to that of type II and TiO_2 which is more than double of TiO_2 photocatalytic activity. Type II shows similar catalytic activity to the conventionally synthesized nanocomposites.[30,31] Hence, type I is better catalyst than the conventionally synthesized and type II nanocomposites. The pretreated TiO_2 and uniform deposition of small size (2-5 nm) AuNPs with similar shape has imparted type I with enhanced photocatalytic dye degrading ability than type II.

Conclusions

In conclusion, our protocol to synthesize the positively charged Au@TiO_2 nanocomposites provides easy, one-pot synthesis, comparatively fast (13 hours), nontoxic, controlled and inexpensive route. Small size (2-5 nm), similar morphology and uniform distribution of AuNPs at the surface of pretreated TiO_2 may provide unique characteristics to Au@TiO_2 nanocomposites (type I) which may be suitable for several applications such as photocatalyst. We performed dye degradation experiments of methyl orange and found that type I shows enhanced photocatalytic activity than type II and TiO_2. In addition, this approach could also be used to synthesize other nanocomposites such as Ag@TiO_2 and Pt@TiO_2.

Acknowledgments. This research was supported by 2011 Yeungnam University research grant.

References

1. (a) Haruta, M.; Yamada, N.; Kobayashi, T.; Iijima, S. *J. Catal.* **1989**, *115*, 301. (b) Haruta, M. *Catal. Today* **1997**, *36*, 153.
2. Bond, G. C.; Sermon, P. A.; Webb, G.; Buchanan, D. A.; Wells, P. B. *J. Chem. Soc. Chem. Commun.* **1973**, *13*, 444.
3. Hashmi, A. S. K.; Hutchings, G. J. *Angew. Chem. Int. Ed.* **2006**, *45*, 896; *Angew Chem* **2006**, *118*, 8064.
4. (a) Corma, A.; Garcia, H. *Chem. Soc. Rev.* **2008**, *37*, 2096. (a) Haruta, M. *Cattech* **2002**, *6*, 102.
5. Bond, G. C.; Thompson, D. T. *Gold. Bull.* **2000**, *33*, 41.
6. Rodriguez, J. A.; Liu, G.; Jirsak, T.; Hrbek, J.; Chang, Z. P.; Dvorak, J.; Maiti, A. *J. Am. Chem. Soc.* **2002**, *124*, 5242.
7. Tabakova, T.; Idakiev, V.; Andreeva, D.; Mitov, I. *Appl. Catal. A* **2000**, *202*, 91.
8. Schwartz, V.; Mullins, D. R.; Yan, W.; Chen, B.; Dai, S.; Overbury, S. H. *J. Phys. Chem. B* **2004**, *108*, 15782.
9. Chen, M.; Goodman, D. W. *Chem. Soc. Rev.* **2008**, *37*, 1860.
10. Primo, A.; Corma, A.; García, H. *Phys. Chem. Chem. Phys.* **2011**, *13*, 886.
11. Li, H.; Bian, Z.; Zhu, J.; Huo, Y.; Li, H.; Lu, Y. *J. Am. Chem. Soc.* **2007**, *129*, 4538.
12. Kamat, P. V. *J. Phys. Chem. C* **2007**, *111*, 2834.
13. Schubert, M. M.; Hackenberg, S.; Veen, A. C. V.; Muhler, M.; Plzak, V.; Behm, R. J. *J. Catal.* **2001**, *197*, 113.
14. Boccuzzi, F.; Chiorino, A.; Manzoli, M. *Mat. Sci. Eng. C* **2001**, *15*, 215.
15. Arabatzis, I. M.; Stergiopoulos, T.; Andreeva, D.; Kitova, S.; Neophytides, S. G.; Falaras, P. *J. Catal.* **2003**, *220*, 127.
16. Tian, Y.; Tatsuma, T. *J. Am. Chem. Soc.* **2005**, *127*, 7632.
17. Zotova, N.; Roberts, F. J.; Kelsall, G. H.; Jessima, A. S.; Hellgardt, K.; Hii, K. K. *Green Chemistry* **2012**, *14*, 226.
18. Grirrane, A.; Corma, A.; García, H. *Science* **2008**, *322*, 1661.
19. Murdoch, M.; Waterhouse, G. I. N.; Nadeem, M. A.; Metson, J. B.; Keane, M. A.; Howe, R. F.; Llorca, J.; Idriss, H. *Nature Chemistry* **2011**, *3*, 489.
20. Silva, C. G.; Rez, R. J.; Marino, T.; Molinari, R.; García, H. *J. Am. Chem. Soc.* **2011**, *133*, 595.
21. Valden, M.; Lai, X.; Goodman, D. W. *Science* **1998**, *281*, 1647.
22. Nguyen, T.-V.; Lee, H.-C.; Yang, O.-B. *Solar Energy Mat. & Solar Cells* **2006**, *90*, 967.
23. May, R. A.; Patel, M. N.; Johnston, K. P.; Stevenson, K. J. *Langmuir* **2009**, *25*, 4498.
24. Jakob, M.; Levanon, H.; Kamat, P. V. *Nano. Lett.* **2003**, *3*, 353.
25. Liu, K.; Zhang, M.; Zhou, W.; Li, L.; Wang, J.; Fu, H. *Nanotechnology* **2005**, *16*, 3006.
26. Yang, Y. F.; Sangeetha, P.; Chen, Y. W. *Int. J. Hydrogen Energy* **2009**, *34*, 8912.
27. Chen, S. F.; Li, J. P.; Qian, K.; Xu, W. P.; Lu, Y.; Huang, W. X.; Yu, S. H. *Nano. Res.* **2010**, *3*, 244.
28. Yates, J. T., Jr. *Surface Science* **2009**, *603*, 1605.
29. Lahiri, D.; Subramanian, V.; Shibata, T.; Wolf, E. E.; Bunker, B. A.; Kamat, P. V. *J. Appl. Phys.* **2003**, *93*, 2575.
30. Zhu, B.; Li, K.; Feng, Y.; Zhang, S.; Wu, S.; Huang, W. *Catalysis Letters* **2007**, *118*, 55.
31. Tian, B.; Zhang, J.; Tong, T.; Chen, F. *Applied Catalysis B: Environmental* **2008**, *79*, 394.
32. Ismail, A. A.; Bahnemann, D. W.; Bannat, I.; Wark, M. *J. Phys. Chem. C* **2009**, *113*, 7429.
33. Anandan, S.; Ashokkumar, M. *Ultrasonics Sonochemistry* **2009**, *16*, 316.
34. Li, J.; Zen, H. C. *Chem. Mater.* **2006**, *18*, 4270.
35. Madler, L.; Stark, W. J.; Pratsinis, S. E. *J. Mater. Res.* **2003**, *18*, 115.
36. Lin, J.; Lin, Y.; Liu, P.; Meziani, M. J.; Allard, L. F.; Sun, Y. P. *J. Am. Chem. Soc.* **2002**, *124*, 11514.
37. (a) Polte, J.; Ahner, T. T.; Delissen, F.; Sokolov, S.; Emmerling, F.; Thünemann, A. F.; Kraehnert, R. *J. Am. Chem. Soc.* **2010**, *132*, 1296. (b) Grabar, K. C.; Freeman, R. G.; Hommer, M. B.; Natan, M. J. *Anal. Chem.* **1995**, *67*, 735.
38. Mie, G. *Ann. Phys.* **1908**, *25*, 377.
39. Tsunoyama, H.; Ichikuni, N.; Sakurai, H.; Tsukuda, T. *J. Am. Chem. Soc.* **2009**, *131*, 7086.
40. Dawson, A.; Kamat, P. V. *J. Phys. Chem. B* **2001**, *105*, 960.
41. Zhou, W.; Liu, Q.; Zhu, Z.; Zhang, J. *J. Phys. D: Appl. Phys.* **2010**, *43*, 035301 (6 pages).
42. DOI: 10.1088/0022-3727/43/3/035301.
43. Othman, S. H.; Rashid, S. A.; Ghazi, T. I. M.; Abdullah, N. *J. of Nanomaterials* **2011**, Article ID 571601, 8 pages, DOI: 10.1155/2011/571601.
44. Othman, S. H.; Rashid, S. A.; Ghazi, T. I. M.; Abdullah, N. *J. of Nanomaterials* **2010**, Article ID 512785, 10 pages, DOI: 10.1155/2010/512785.
45. Subramanian, V.; Wolf, E. E.; Kamat, P. V. *J. Am. Chem. Soc.* **2004**, *126*, 4943.